

Iterative execution of discrete and inverse discrete Fourier transforms with applications for signal denoising via sparsification

H. Robert Frost¹

¹*Department of Biomedical Data Science
Geisel School of Medicine
Dartmouth College
Hanover, NH 03755, USA
rob.frost@dartmouth.edu*

Abstract

We describe a family of iterative algorithms that involve the repeated execution of discrete and inverse discrete Fourier transforms. One interesting member of this family is motivated by the discrete Fourier transform uncertainty principle and involves the application of a sparsification operation to both the time domain and frequency domain data with convergence obtained when time domain sparsity hits a stable pattern. This sparsification variant has practical utility for signal denoising, in particular the recovery of a periodic spike signal in the presence of Gaussian noise. General convergence properties and denoising performance are demonstrated using simulation studies. We are not aware of prior work on such iterative Fourier transformation algorithms and are posting this short paper in part to solicit feedback from others in the field who may be familiar with similar techniques.

1 General problem statement

We consider the class of iterative discrete Fourier transform [1] techniques described by Algorithm (1). The structure of this algorithm is broadly motivated by iterative optimization methods such as the expectation-maximization (EM) algorithm [2]. The family of algorithms we consider take a real-valued vector \mathbf{x} as input and then repeatedly perform the following sequence of actions:

- Execute a time domain function $h()$ on \mathbf{x} .
- Perform a discrete Fourier transform on the output of $h()$.
- Execute frequency domain function $g()$ on the complex vector output by the discrete Fourier transform.

- Transform the output of $g()$ back into the time domain via the inverse discrete Fourier transform.

Convergence of the algorithm is determined by a function $c()$ that compares the output of $h()$ on the current iteration to the version from the prior iteration. When convergence is obtained, the output from the last execution of $h()$ is returned.

For this general family of algorithms, a key question relates to what combinations of $h()$, $g()$, and $c()$ functions and constraints on \mathbf{x} enable convergence. Of course, if both $h()$ and $g()$ are the identify function, then convergence occurs after single iteration and the entire algorithm operates as the identify function. We are therefore interested in scenarios involving non-trivial convergence to a value that is relevant for a specific data analysis application, e.g., a denoising or optimization problem. In general, we will assume that neither $h()$ nor $g()$ are the identify function and that the number of iterations until convergence, i_c , is a function of \mathbf{x} , i.e., if \mathbf{x} is a random vector, then i_c is a random variable.

2 Iterative convergence under sparsification

An interesting subclass of the general iterative method detailed in Algorithm 1 involves the use of sparsification functions for both $h()$ and $g()$ with $c()$ identifying convergence when a stable sparsity pattern is achieved in the output of $h()$. Iterating between time domain and frequency domain sparsification is motivated by the discrete Fourier transform uncertainty principal [3], which constrains the total number of zero values in the time domain data and frequency domain representation generated by a discrete Fourier transform. Attempts to induce sparsity in one domain will reduce sparsity in the other domain with the implication that setting both $h()$ and $g()$ to sparsification functions will not simply result in the generation of a vector of all 0 elements. Instead, for scenarios where the iterative algorithm converges, the solution will represent a stable compromise between time and frequency domain sparsity.

We can explore the general convergence properties of Algorithm 1 using sparsification functions for $h()$ and $g()$ via the following simulation design:

- Set \mathbf{x} to a length n vector of $\mathcal{N}(0, 1)$ random variables.
- Define $h()$ to generate a sparse version of \mathbf{x} where the proportion p of elements with the smallest absolute values are set to 0.
- Define $g()$ to generate a sparse version of \mathbf{w} where the proportion p of complex coefficients with the smallest magnitudes are set to $0 + 0i$.
- Define $c()$ to identify convergence when the indices of 0 values in the output of $h()$ are identical on two sequential iterations.
- The discrete and inverse discrete Fourier transforms are realized using the Fast Fourier Transform.

Algorithm 1 Iterative application of discrete Fourier and inverse Fourier transforms

Inputs:

- $\mathbf{x} \in \mathbb{R}^n$ ▷ Input data
- i_m ▷ The maximum number of iterations

Outputs:

- $\mathbf{y} \in \mathbb{R}^n$ ▷ Output data
- i_c ▷ Number of iterations completed

Notation:

- Let $h()$ be a time domain function that accepts and returns length n vectors of real numbers.
- Let $g()$ be a frequency domain function that accepts and returns length n vectors of complex numbers.
- Let $c()$ be a convergence function that accepts two length n vectors of real numbers and returns a boolean indicating convergence.

```
1:  $i = 1$  ▷ Initialize iteration index
2:  $\mathbf{x}_0 = \mathbf{x}$  ▷ Initialize  $\mathbf{x}_i$ 
3: while  $i \leq i_m$  do
4:    $\mathbf{x}_i^* = h(\mathbf{x}_{i-1})$  ▷ Apply  $h()$  to  $\mathbf{x}_{i-1}$ 
5:   if  $c(\mathbf{x}_i^*, \mathbf{x}_{i-1}^*)$  then ▷ Check for convergence
6:     break ▷ If convergence conditions met, stop the iteration
7:    $\mathbf{w}_i = dft(\mathbf{x}_i^*)$  ▷ Compute discrete Fourier transform of  $\mathbf{x}_i^*$ 
8:    $\mathbf{w}_i^* = g(\mathbf{w}_i)$  ▷ Apply  $g()$  to complex vector  $\mathbf{w}_i$ 
9:    $\mathbf{x}_i = dft^{-1}(\mathbf{w}_i^*)$  ▷ Compute inverse discrete Fourier transform of  $\mathbf{w}_i^*$ 
10:   $i = i + 1$  ▷ Increment iteration index
   return  $(\mathbf{x}_i^*, i)$  ▷ Return the output of the final execution of  $h()$ 
```

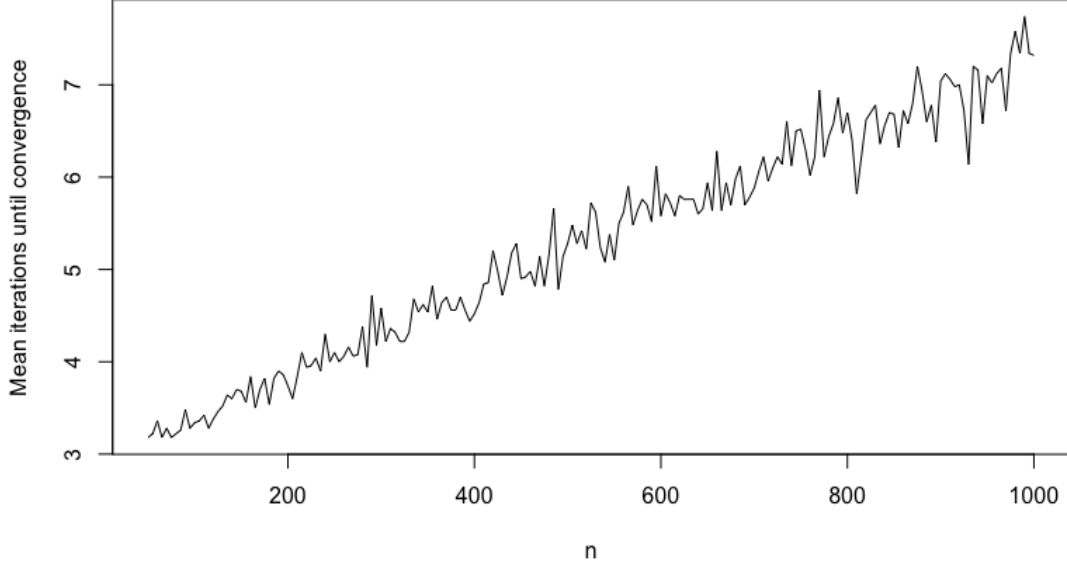


Figure 1: Mean iterations until convergence for random length n vectors of $\mathcal{N}(0, 1)$ random variables and $h()$ and $g()$ functions that rank order the elements according to absolute value or magnitude and set the bottom 50% to 0. Convergence is based on repeating the same pattern of sparsity after execution of $h()$ on two sequential iterations.

Following this design, we applied the algorithm to 50 simulated \mathbf{x} vectors for each distinct n value in the range from 50 to 1,000 using the sparse proportion of $p = 0.5$ and the maximum number of iterations $i_m = 50$. Figure 1 below displays the mean number of iterations until convergence as a function of n . Figure 2 illustrates the results from a similar simulation that used a fixed n of 500 and sparse proportion value ranging from 0.1 to 0.9. For all of the tests visualized in Figures 1 and 2, the algorithm converged to a stable pattern of sparsity in \mathbf{x} . Not surprisingly, the number of iterations required to achieve a stable sparsity pattern increased with the growth in either n or p . If $h()$ and $g()$ are changed to set all elements with absolute value or magnitude below the mean to 0 (see simulation design in Section 3), the relationship between mean iterations until convergence and n is similar to that shown in Figure 1. Changing the generative model for \mathbf{x} to include a non-random periodic signal (e.g., sinusoidal signal or spike signal) also generates similar convergence results.

3 Detection of spike signals using iterative convergence

To assess the practical utility of a sparsification version of Algorithm 1 for signal denoising, we used the following simulation design:

- Set \mathbf{x} to the combination of a periodic spike signal \mathbf{s} and Gaussian noise $\boldsymbol{\varepsilon}$, $\mathbf{x} = \mathbf{s} + \boldsymbol{\varepsilon}$,

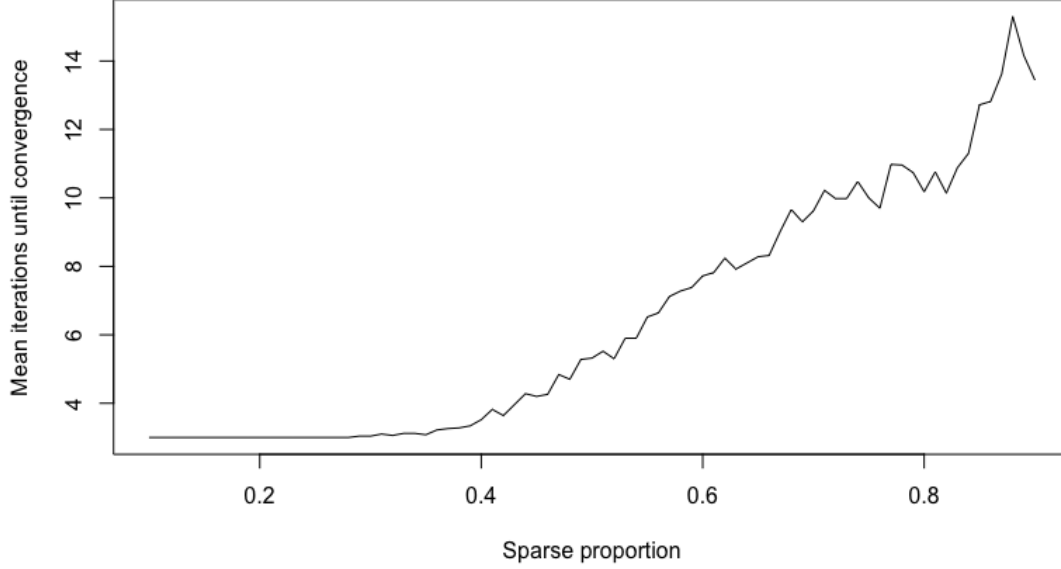


Figure 2: Mean iterations until convergence for random length 500 vectors of $\mathcal{N}(0, 1)$ random variables. For these results $h()$, $g()$, and $c()$ have similar definitions as detailed for Figure 1. In this case, n was fixed at 500 and the sparsity proportion varied between 0.1 and 0.9.

with:

- Elements $s_i, i \in (1, \dots, n)$ of \mathbf{s} set to 0 for all $i \neq a\lambda$ and generated as $U(\alpha_{min}, \alpha_{max})$ random variables for $i = a\lambda, a \in (1, \dots, b)$ where b is the total number of cycles and $\lambda \geq 1$ is the period.
- Elements ε_i of $\boldsymbol{\varepsilon}$ are generated as independent random variables with distribution $\mathcal{N}(0, \sigma^2)$.
- Define $h()$ to generate a sparse version of \mathbf{x} where all elements $x_i \leq 1/n \sum_{j=1}^n |x_j|$ are set to 0.
- Define $g()$ to generate a sparse version of \mathbf{w} where all elements $w_i \leq 1/n \sum_{j=1}^n |w_j|$ are set to $0 + 0i$ (here the $||$ operation represents the magnitude of the complex number w_j).
- Define $c()$ to identify convergence when the indices of 0 values in the output of $h()$ are identical on two sequential iterations.

Figure 3 shows an example of \mathbf{x} generated according to this simulation model with $\alpha_{min} = \alpha_{max} = 2.5, b = 16, \lambda = 8$ and $\sigma^2 = 0.5$. For this specific example, the method converges in seven iterations and perfectly recovers the periodic spike signal.

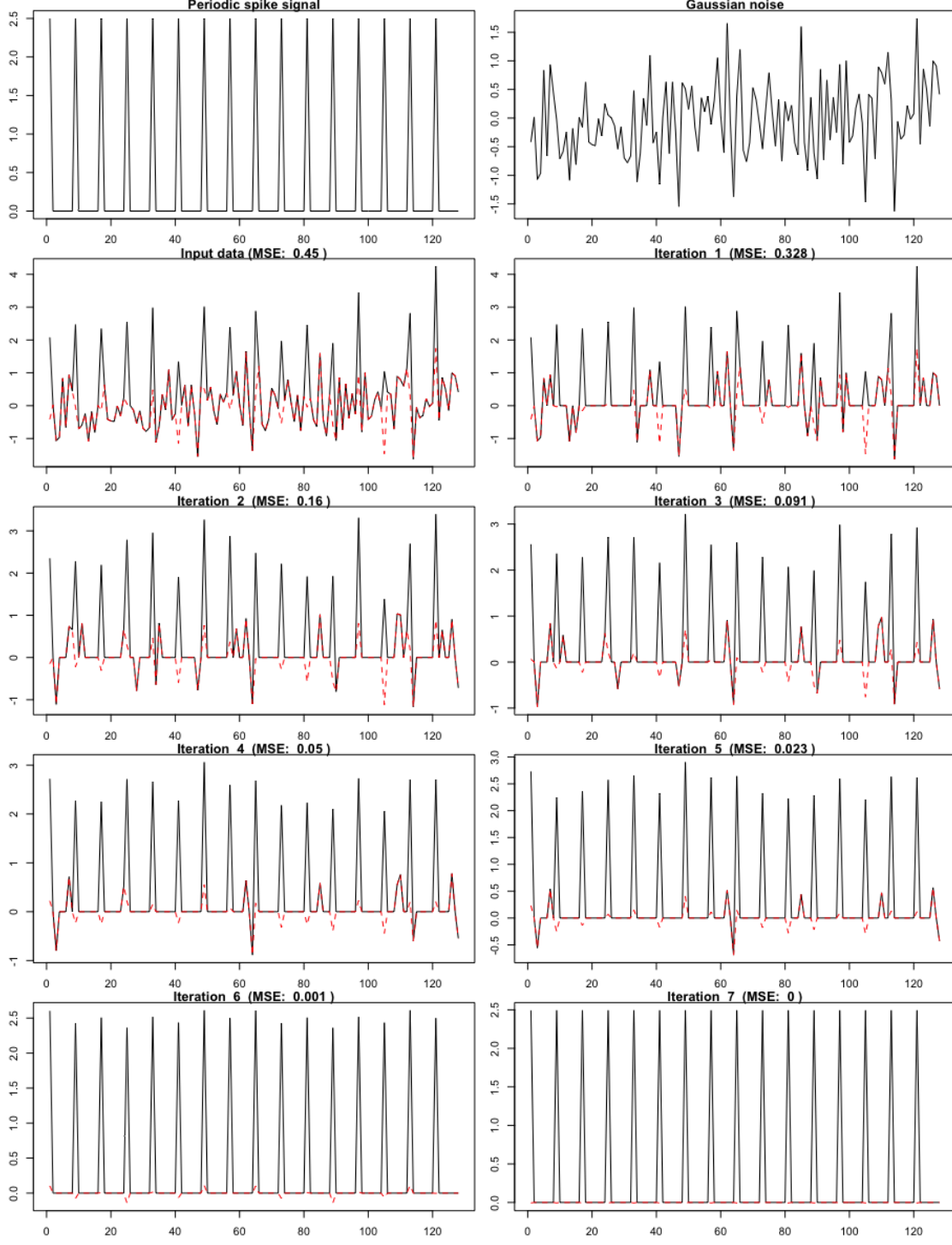


Figure 3: Results from the application of Algorithm 1 to an \mathbf{x} vector simulated according to the model detailed in Section 3 with $\alpha_{min} = 2.5, \alpha_{max} = 2.5, b = 16, \lambda = 8$ and $\sigma^2 = 0.5$. The top panels show the periodic spike signal and Gaussian noise. The remaining panels show the input data and output from the $h()$ sparsification function after each iteration of the algorithm with the error relative to the spike signal captured as a dashed red line and quantified via the mean squared error.

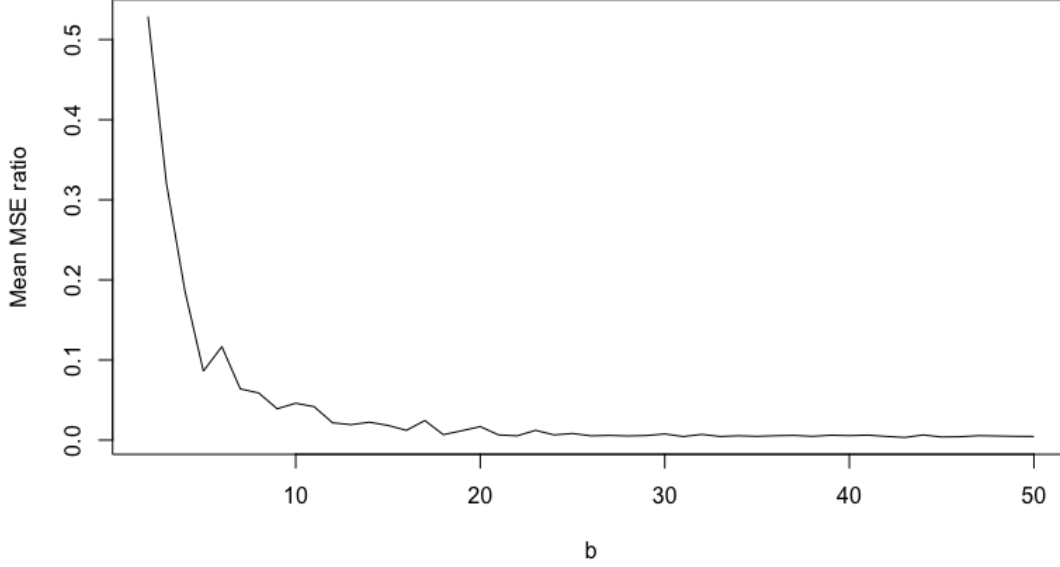


Figure 4: Average mean squared error (MSE) ratio relative to the number of cycles, b , captured in the input \mathbf{x} vector. The MSE ratio is computed as MSE_c/MSE_1 where MSE_c represents the MSE after convergence and MSE_1 represents the MSE after the first execution of $h()$ on the input \mathbf{x} .

To more broadly characterize signal recovery for this simulation design, multiple \mathbf{x} vectors were generated for different values of α_{min} , α_{max} , b , λ , and σ^2 . Figure 4 shows the relationship between the MSE ratio achieved on converge averaged across 50 simulated \mathbf{x} vectors and the number of cycles, b , captured in \mathbf{x} . The MSE ratio is specifically computed as MSE_c/MSE_1 where MSE_c is the mean squared error (MSE) between the output of the method after convergence and the spike signal \mathbf{s} and MSE_1 is the MSE for the output from the first execution of $h()$. For this simulation design, the average MSE ratio is very close to 0 for $b \geq 20$, which reflects near perfect recovery of the input periodic spike signal. Figure 5 captures the association between the average MSE ratio and the number of iterations completed by the algorithm (b was fixed at 20 for this simulation). These results demonstrate that signal recovery consistently improves on each iteration of the algorithm with the lowest MSE achieved upon convergence. Figure 6 captures the association between the average MSE ratio achieved on convergence and Gaussian noise variance (b was fixed at 20 for this simulation). These results demonstrate the expected increase in signal recovery error with increase noise variance and, importantly, show that the method still achieves improved noise recovery relative to just a single execution of $h()$ at high levels of noise.

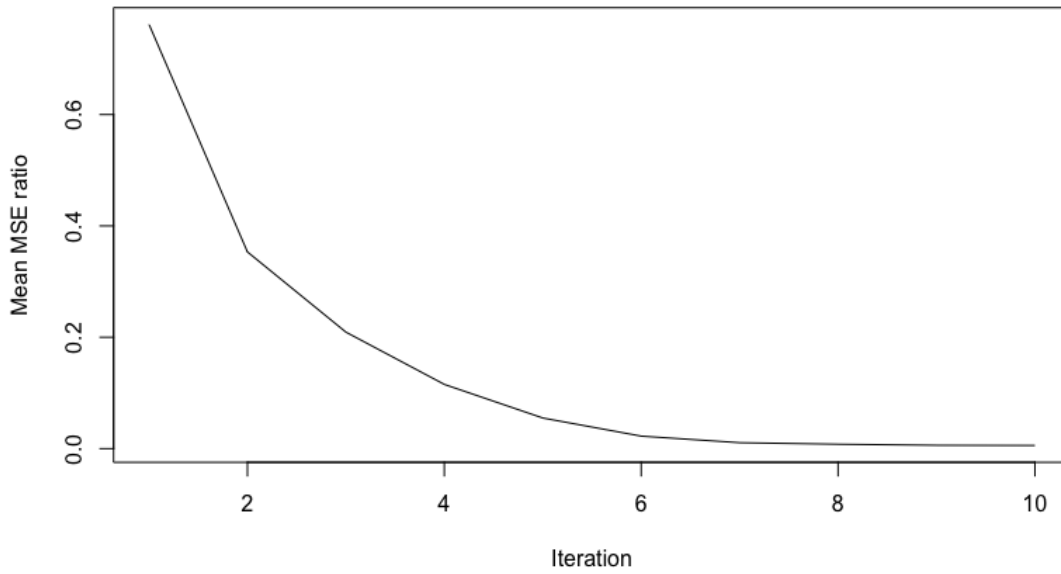


Figure 5: Average MSE ratio after each iteration of the algorithm.

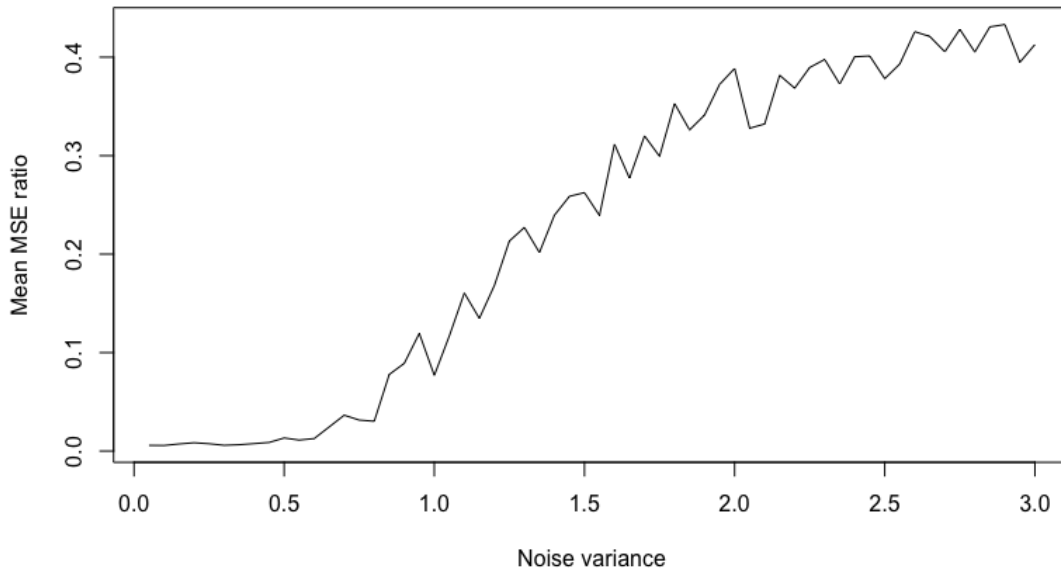


Figure 6: Average mean squared error (MSE) ratio relative to the variance of the Gaussian noise, σ^2 , added to the periodic spike signal.

4 Next steps

We wrote this brief paper to both document the idea and solicit feedback from others in the field regarding any prior work that may have been done on the iterative application of Fourier and inverse Fourier transforms. We are currently working on a more comprehensive manuscript describing this technique that includes the exploration of necessary conditions for convergence, theoretical basis for the denoising performance shown in Section 3, performance on a broader range of signal and noise patterns and $h()$, $g()$ and $c()$ functions, and comparison against existing denoising techniques.

Acknowledgments

This work was funded by National Institutes of Health grants R35GM146586 and R21CA253408. We would like to thank Anne Gelb for the helpful discussion.

References

- [1] Ronald N Bracewell. *The Fourier transform and its applications*. McGraw Hill, Boston, 3rd ed edition, 2000.
- [2] A. P. Dempster, N. M. Laird, and D. B. Rubin. Maximum likelihood from incomplete data via the em algorithm. *Journal of the Royal Statistical Society. Series B (Methodological)*, 39(1):1–38, 1977.
- [3] David L. Donoho and Philip B. Stark. Uncertainty principles and signal recovery. *SIAM Journal on Applied Mathematics*, 49(3):906–931, 1989.